Effectiveness of Surface Electromyography in Pattern Classification for Upper Limb Amputees

Carl Peter Robinson, Baihua Li *, Qinggang Meng, Matthew Pain
Loughborough University, Loughborough, UK LE11 3TU
First Author: C.P.Robinson@lboro.ac.uk
* Corresponding Author b.li@lboro.ac.uk

ABSTRACT
This study was undertaken to explore 18 time domain (TD) and time-frequency domain (TFD) feature configurations to determine the most discriminative feature sets for classification. Features were extracted from the surface electromyography (sEMG) signal of 17 hand and wrist movements and used to perform a series of classification trials with the random forest classifier. Movement datasets for 11 intact subjects and 9 amputees from the NinaPro online database repository were used. The aim was to identify any optimum configurations that combined features from both domains and whether there was consistency across subject type for any standout features. This work built on our previous research to incorporate the TFD, using a Discrete Wavelet Transform with a Daubechies wavelet. Findings report configurations containing the same features combined from both domains perform best across subject type (TD: root mean square (RMS), waveform length, and slope sign changes; TFD: RMS, standard deviation, and energy). These mixed-domain configurations can yield optimal performance (intact subjects: 90.98%; amputee subjects: 75.16%), but with only limited improvement on single-domain configurations. This suggests there is limited scope in attempting to build a single absolute feature configuration and more focus should be put on enhancing the classification methodology for adaptivity and robustness under actual operating conditions.

CCS Concepts
• **Computing methodologies→Machine learning** • **Computing methodologies→Feature selection** • *Human-centered computing~Interaction techniques.*

Keywords
Machine Learning; Feature Extraction; Classification; Surface Electromyography; Myoelectric Control.

1. INTRODUCTION
For several decades, myoelectric control systems have been endorsed for transradial amputees to regain a satisfactory daily life experience. They provide an affordable, amenable means of operation using surface electromyography (sEMG) to capture the electrical activity from muscle innervation. Despite great advances in commercial prostheses there remains a gap with the control strategies put forward to drive them [18]. The majority are sequential by nature (i.e. one full movement followed by another), often using a coactivation switch to cycle through a series of available mechanical actions [6]. Pattern recognition systems are slowly making their way onto the market (http://www.coaptengineering.com), exploiting machine learning techniques to perform specific movements. However, both approaches currently do not provide intuitive control and accurate, reliable operation.

Considering pattern recognition, the extraction of appropriate features concentrates on deriving pertinent structural characteristics from the EMG signal. This is distinctly important, aiming for the best separation between physical gestures [14]. The cogency of this assertion is seen in the considerable influence feature choice has on classification results [10]. EMG features are divided into three categories: time domain (TD), frequency domain (FD) and time-frequency domain (TFD). TD features provide low-cost measurements, evaluating the EMG signal amplitude. FD features rely on an initial remodelling process, using a Fourier Transform to describe signal components, or to ascertain its power spectral density. Both domains suffer from deficiencies. The TD does not account for the non-stationarity of the EMG signal, thus missing important statistical information. The FD may misrepresent the signal through leakage or fail to capture changes in signal content over time. TFD features can overcome these shortfalls, combining the time element with a frequency transform to specify the energy concentration for each frequency present at a particular time instant [13]. Using wavelet analysis, a signal is represented as a series of oscillatory functions of finite duration (wavelets) by decomposing it using a wavelet transform. It can therefore be expressed as a linear combination of these functions with wavelet coefficients giving a compact representation of the signal's energy [12]. Significant work has been done in recent decades, to elucidate ideal feature choice [14], [15], [16]. Wavelet analysis has also been explored, incorporated into a neural network to maximise feature extraction and learning when using a limited number of EMG sensors [5], combined with principal component analysis to improve grasp recognition for rehabilitation [10], and compared with FFT for muscle fatigue prediction [4]. This paper expands on our previous work that investigated 7 TD feature configurations against a series of online datasets, examining TFD potential with

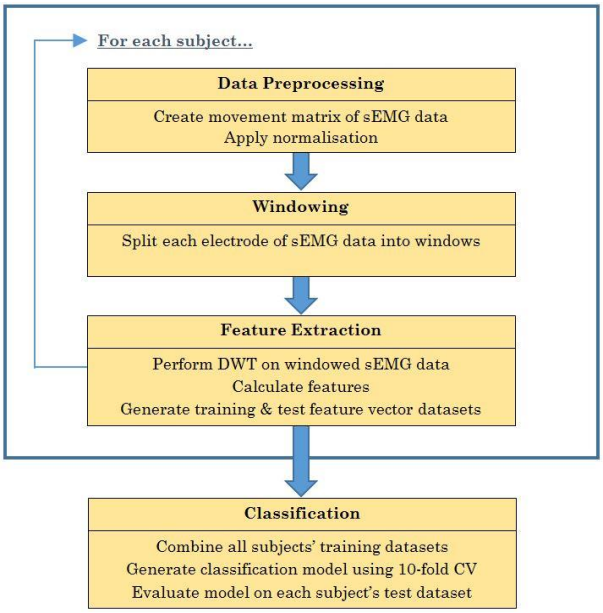

Figure 1. Experiment process flow using DWT features.

17 human hand and wrist movements, using a discrete wavelet transform (DWT) to decompose the sEMG signal. For this reason, features extracted using this process are referred to as DWT features. Classification trials using a random forest (RF) classifier are performed on both intact and amputee subject data over 4 experiments. In all, comparisons of 18 feature configurations are made: TD-only, DWT-only and TD combined with DWT.

2. METHOD

2.1 Preprocessing and Windowing

The experimental procedure followed the same protocol detailed previously [17]. It is summarised here for convenience and depicted in Fig. 1. Intact and amputee data were downloaded from the NinaPro project (http://ninapro.hevs.ch), and Exercise B's 17 hand and wrist movements were chosen. The first 11 datasets for healthy, intact subjects from Database 2 and 9 amputee subject datasets from Database 3 were used. 12 Delsys Trigno wireless electrodes (Delsys, Inc, www.delsys.com) were used to acquire the sEMG data. Eight electrodes were attached around the right forearm, at a fixed distance from the radio-humeral joint, two were fixed to the main activity spots of the anterior and posterior of the forearm, and two more placed on the biceps brachii and triceps brachii. All movements were repeated 6 times consecutively, each lasting approximately 5 seconds, plus a 3-second rest period where a rest posture was assumed. Data was acquired at a 2 KHz sampling rate, cleaned and relabelled suitably
before being made available online. A thorough account of the NinaPro experiment is available here [3].
An in-house MATLAB program separated movement repetitions into a matrix of time-ordered sEMG voltage data from the 12 electrodes. Each movement's data was split such that repetitions 1, 3, 4, and 6 were allocated to a training set and repetitions 2 and 5 to a test set. All data were normalised to have zero mean and unit standard deviation [3]. A 256ms sliding window was employed, as per our previous work, to segment the data. The increment was set at 10 ms to ensure a densely packed array of windows but a moving average was applied to the process to prevent unmanageable file sizes.

2.2 Wavelet Analysis

This undertaking focused on producing DWT features. Prior to feature extraction, a discrete wavelet transform (DWT) was performed on the sEMG signal. Data was processed through multiple levels using a filter-bank of low-pass and highpass filters that decomposed the signal into approximation and detail subbands, respectively (Fig. 2). At each level, approximation coefficients corresponding to the low frequency signal components were generated, using a set of discretised wavelet functions, based on a mother wavelet $\psi(t)$:

$$\boldsymbol{\psi_{j,k}}(\mathbf{t}) = \frac{1}{\sqrt{s_0^j}}\boldsymbol{\psi}\left(\frac{t - k\tau_0 s_0^j}{s_0^j}\right), \boldsymbol{j,k} \in \mathbb{Z} \qquad (1)$$

where s_0 is a fixed scale parameter, τ_0 is a translation factor, j is used to adjust the scale, k controls the translation and t refers to time. To provide dyadic scaling and translation and the required discretisation, s_0 is set to 2 and τ_0 to 1. Additionally, a set of scaling functions – stretched and translated versions of a base scaling function $\varphi(t)$, using the same method as (1) – were used to generate detail coefficients representing the signal's high frequency components. The current approximation subband was used to yield the next level of approximation and detail subbands until the desired level was reached. Corresponding subband coefficients were generated as follows:

$$\boldsymbol{c_j} = \frac{1}{\sqrt{s_0^2}}\sum_n \langle \boldsymbol{\varphi_{j,k}}, \boldsymbol{\varphi_{j-1,n}} \rangle \boldsymbol{c_{j-1}} \qquad (2)$$

$$\boldsymbol{d_j} = \frac{1}{\sqrt{s_0^2}}\sum_n \langle \boldsymbol{\psi_{j,k}}, \boldsymbol{\psi_{j-1,n}} \rangle \boldsymbol{d_{j-1}} \qquad (3)$$

where c_j and d_j are the approximation and detail coefficients respectively, for the current level, specified by n. This repeated process removes redundancy in the coefficient data, making the DWT more efficient and faster than a continuous wavelet transform (CWT) [9], hence its choice here.
It is imperative the most relevant wavelet is chosen for the DWT, to maximise the transform. The Daubechies db7 wavelet was selected based on related DWT usage with EMG [3] and comparison with the signal characteristics of the EMG datasets in use. For decomposition, 3 and 4 levels are common, cited as optimum [3] [12]. Four levels were selected, implying four detail subbands, and a corresponding 4th level approximation subband. The DWT was executed using built-in MATLAB functions and returned a vector of wavelet coefficients for each subband (an example of 4 levels of detail subband coefficient data is given in Fig. 3).

2.3 Feature Extraction

Features were chosen according to previous research [17] [8] [10]. TD features were extracted from each time window and DWT features from the transformed time window's subband coefficient data.

2.3.1 Configurations C1 to C4 (Table 2)

A feature vector v_t of extracted DWT features for all 12 electrodes E was created, giving a 300-value feature vector for one time window t:

$$\begin{aligned}\mathbf{v_t} &= \{f_{1,1}^1, f_{1,2}^1, \ldots, f_{2,1}^1, f_{2,2}^1, \ldots, f_{1,1}^2, \ldots, f_{b,h}^e\}, \\ &= \{f_{b,h}^e | b = 1, \ldots, B, B = 5; h = 1, \ldots, H, H = 5; \\ &\quad e = 1, \ldots, E, E = 12\}\end{aligned} \qquad (4)$$

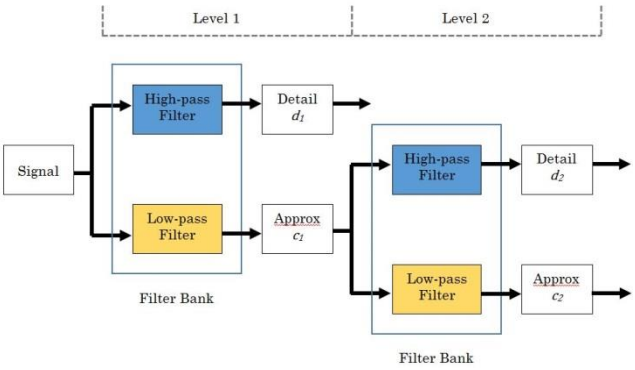

Figure 2. Example of a 2-level DWT decomposition process.

Table 1. Construction of DWT Features.

Feature	Equation
Root Mean Square of coeffs	$\text{RMSCO} = \sqrt{\frac{1}{N}\sum_{i=1}^{N} x_i^2}$
Standard Dev of coeffs	$\text{STDCO} = \sqrt{\frac{1}{N}\sum_{i=1}^{N} x_i^2\,(x_i - \bar{x})^2}$
Energy of coeffs	$\text{ENGCO} = \sum_{i=1}^{N} \lvert x_i \rvert^2$
Mean Abs Value of coeffs	$\text{MAVCO} = \frac{1}{N}\sum_{i=1}^{N} \lvert x_i \rvert$
Mean Power of coeffs	$\text{MEANPWR} = \sum_{i=1}^{N} x_i^2$
where N is number of coefficients and x indicates c and d	

where *t* refers to one time window, *e* is an electrode, *f* is the *h*th feature value at subband *b* and electrode index *e*, *B* is the total subbands, and *H* is the number of DWT features per subband. For all windows, a time-ordered feature vector matrix composed [17].

The feature selection tool in the WEKA software application, version 3.8 (http://www.cs.waikato.ac.nz/ml/weka) was used to evaluate and rank the features with an attribute evaluator and associated search method. This determined their suitability in relation to each class label and from the results, four feature configurations were derived, C1 to C4 (Table 2).

2.3.2 Configurations C5 to C11 (Table 4)

For amputees, both TD and DWT experiments were undertaken. TD and DWT feature configurations are outlined in Table 4. The same DWT settings and process were applied in this experiment, as above.

2.3.3 Configurations C12 to C18 (Table 5)

Two further experiments were performed, one on the 11 intact subjects, another using the 9 amputee subjects. Both combined specific TD and DWT features, attempting to optimise configurations, producing an updated version of the feature vector in (4) to include TD features for each electrode:

$$\begin{aligned}\mathbf{v_t} &= \{f_1^1, f_i^e, \ldots, f_{1,1}^1, \ldots, f_{b,h}^e\}, \\ &= \{f_i^e \mid i = 1, \ldots, I, I = 4\}\end{aligned} \quad (5)$$

where *i* is a single TD feature value and *I* is the total number of TD features.

A feature selection process was undertaken to find the most relevant features (Table 3). Information Gain and Correlation

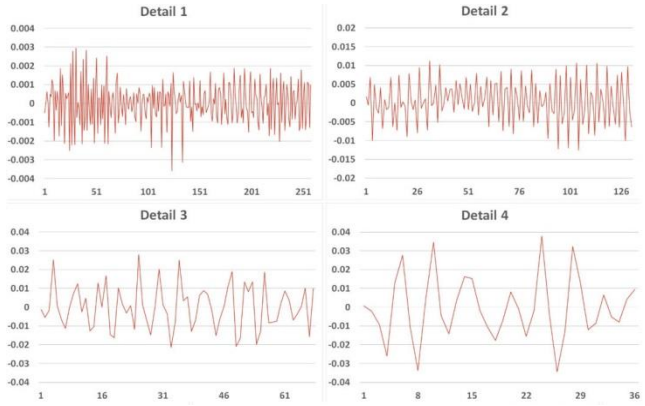

Figure 3. Coefficient data for detail subbands to four levels, generated as a result of performing a DWT on one window of sEMG data, in this case the third repetition of movement 2.

Table 2. DWT Features and configurations used in experiment 1 (11 intact subjects).

Feature	C1	C2	C3	C4
Root Mean Square (RMSCO)	✓	✓	✓	✓
Standard Dev. (STDCO)	✓	✓	✓	
Energy (ENGCO)	✓			
Mean Abs. Value (MAVCO)		✓		✓
Mean Power (MEANPWR)				✓

(using Pearson's correlation coefficient) evaluation types used the Ranker search method while Decision Tree, Random Forest and Logistic Regression were selected under the WrapperSubsetEval learner method and were tested using cross validation and a Best First search. Results were ranked according to feature efficacy in relation to the classes. Using these results and the performance of features in previous experiments, 3 feature configurations were created for intact subjects and 4 amputees, each consisting of between 4 and 6 features (Table 5).

2.4 Classification

A series of classification models were created using WEKA with a between-subject strategy, using all subjects' training data, then performing evaluation with each individual subject's test data, collating results accordingly. The random forest classifier was chosen, having previously performed best among support vector machine, multilayer perceptron and k-nearest neighbour [17]. A 10-fold cross validation was used to provide estimated performance and produce the final models for each experiment.

3. Results and Discussion

Classification rate (CR) was used to evaluate classifier performance, calculated by dividing the number of correctly classified instances over the total instances, producing an accuracy value to indicate correctly identified hand movements:

$$\frac{\boldsymbol{CorrectlyClassifiedInstances}}{\boldsymbol{TotalNumberOfInstances}} \times \mathbf{100}\% \quad (6)$$

3.1.1 Experiment 1

For the 11 intact subjects DWT experiment, configuration C1 produced the best average accuracy, garnering 90.59%. However,

Table 3. WEKA attribute selection methods and features for configurations C12 to C18 (TD and DWT features for intact and amputee subjects). Features identified in footnote[1]

Intact Subjects	
Evaluator	**Ranked Attribute**
Information Gain	2, 1, 4, 3, 6, 7, 5, 8, 9
Correlation	2, 5, 6, 8, 1, 4, 3, 9, 7
Decision Tree	3, 2, 1, 4, 6, 7, 5, 9, 8
Random Forest	3, 2, 1, 8, 4, 9, 7, 6, 5
Logistic Regression	5, 4, 7, 2, 1, 3, 6, 9, 8
Amputee Subjects	
Evaluator	**Ranked Attribute**
Information Gain	2, 5, 6, 7, 8, 1, 4, 3, 9
Correlation	7, 9, 3, 6, 5, 8, 2, 4, 1
Decision Tree	2, 4, 6, 5, 3, 1, 7, 8, 9
Random Forest	2, 1, 3, 4, 6, 9, 5, 8, 7
Logistic Regression	9, 1, 7, 6, 5, 2, 3, 4, 8

[1]1: RMS, 2: WL, 3: SSC, 4: MAV, 5: RMSCO, 6: STDCO, 7: ENGCO, 8: MAVCO, 9: MEANPWR

the four configurations produced very similar results. This suggests that choice of feature combination, at least from the chosen set, had limited bearing on final classification accuracy. The chart in Fig. 4 shows classification results for each subject, for all configurations, and provides the most interesting detail. Specifically, it varied as to which feature configuration produced the best results for each subject, there was no one outstanding configuration. The intact data might be quite ideal among subjects and the sample size of 11 subjects is small, so there may be lack of sufficient data variation for effective analysis.

3.1.2 Experiment 2

Initial trials with all 11 amputee subjects in Database 3, from the NinaPro repository, produced difficulties in experiment procedure, due to 2 subjects using fewer electrodes than the standard 12 used by all other amputees [3]. For this reason, only the 9 amputee subjects with sEMG data for 12 electrodes were used in this research. Classification accuracy results for amputee TD and DWT configurations are presented in Table 4. The best TD configuration was C5 with 73.45% (composed of WL, RMS and SSC features), notable due to high performance in our previous work [17], producing a consistent performance across subject type. It was 1.18% better than the next best configuration, C7 with 72.27%, interestingly only containing two features (RMS and WL) and outperforming the 71.90% of the three-featured C6 configuration. This reinforced previous research of RMS and WL feature selection for sEMG pattern recognition [16] [2]. DWT configurations produced higher accuracy results than their TD counterparts by an average of 1.75%. The C8 configuration, consisting of RMS, STDCO and ENGCO features, performed best with 74.37%. This was 0.30% better than C9, which substituted the ENGCO feature with MAVCO. There was little variability between results again, although more than with intact subjects' DWT results. For amputees, best and worst TD configurations gave a difference of 1.55% in accuracy and 1.47% for best and worst DWT

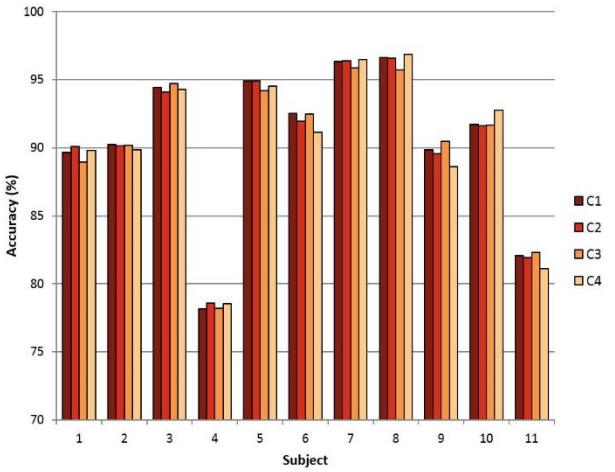

Figure 3. Average classification accuracy results for DWT configurations C1 to C4 (Table 2) for 11 intact subjects, as part of experiment 1.

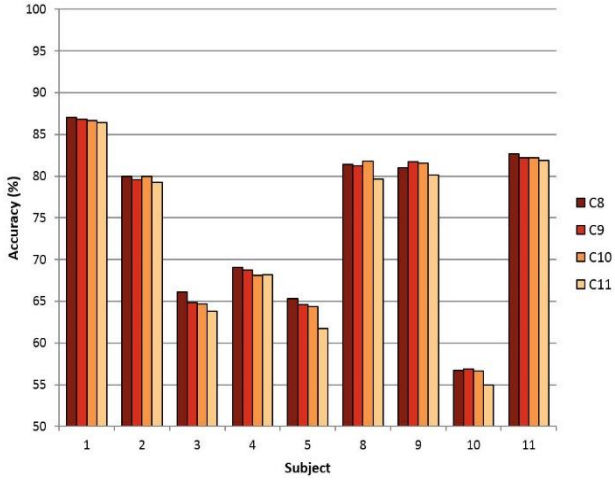

Figure 2. Average classification accuracy results for configurations C8 to C11 (Table 4) for 9 amputee subjects, as part of experiment 2.

configurations. Results here imply feature choice isn't as important, but more the set-up and application of the DWT transform process. It could be that feature choice was approaching optimum but further investigation would be needed to verify this and it seems unlikely. Fig. 5 shows individual subject results for all 4 configurations. This time we see a slight preference for C8, although not for 3 of the subjects, which equates to a third of the group. Although this test population is small, it would be interesting to see if such percentages carried through to larger groups, suggesting again that no one feature configuration is ideal for every end user of a system.

3.1.3 Experiments 3 and 4

Table 5 shows the results of combining domain features for intact and amputee subjects. The best performance for intact subjects came from configuration C14 (RMS, WL, SSC from TD, and STDCO, ENGCO from DWT), achieving 90.98%. But the difference between all 3 mixed-domain configurations only varied by 0.32%. It is also better than both previous best-performing TD and DWT single-domain configurations (90.57% and 90.59%, respectively), but then so are C12 and C13. This shows that combining TD and DWT features increases overall classification

accuracy, but not by any great amount, at least for intact subjects. For amputee subjects, C17 achieved 75.16% accuracy, consisting of the same features as C14. However, the difference between the second and third best configurations is even more negligible than it was for intact subjects (= 0.04% for C15 and = 0.08% for C18).

Table 4. Feature configurations for TD (C5 to C7) and DWT (C8 to C11) used in experiment 2 (9 amputee subjects) and their average classification accuracy results.

TD Feature	**C5**	**C6**	**C7**	
Root Mean Square (RMS)	✓	✓	✓	
Waveform Length (WL)	✓	✓	✓	
Slope Sign Changes (SSC)	✓			
Mean Abs. Value (MAV)		✓		
Accuracy (%)	73.45	71.90	72.27	
DWT Feature	**C8**	**C9**	**C10**	**C11**
Root Mean Square (RMSCO)	✓	✓	✓	✓
Standard Dev (STDCO)	✓	✓	✓	
Energy (ENGCO)	✓			
Mean Abs. Value (MAVCO)		✓		✓
Mean Power (MEANPWR)				✓
Accuracy (%)	74.37	74.07	74.00	72.90

Table 5. Combined TD and DWT feature configurations (C12 to C18) used in experiments 3 and 4 (11 intact and 9 amputee subjects) and their average classification accuracies.

TD Feature	**C12**	**C13**	**C14**	
Root Mean Square (RMS)	✓	✓	✓	
Waveform Length (WL)	✓	✓	✓	
Slope Sign Changes (SSC)	✓		✓	
Standard Dev. (STDCO)	✓	✓	✓	
Energy (ENGCO)	✓	✓	✓	
RMS of coeffs (RMSCO)	✓			
Accuracy (%)	90.87	90.66	90.98	
DWT Feature	**C15**	**C16**	**C17**	**C18**
Root Mean Square (RMS)	✓	✓	✓	✓
Waveform Length (WL)	✓	✓	✓	
Slope Sign Changes (SSC)	✓		✓	
Mean Abs. Value (MAV)				✓
Standard Dev. (STDCO)	✓	✓	✓	✓
Energy (ENGCO)	✓	✓	✓	✓
RMS of coeffs (RMSCO)	✓			✓
Accuracy (%)	75.11	74.82	75.16	75.08

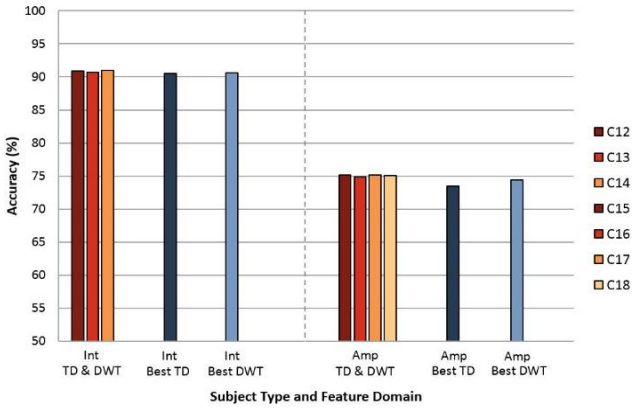

Figure 4. Average classification accuracy results for configurations C12 to C18 (Table 5) for 11 intact and 9 amputee subjects, alongside best performing TD and DWT configurations from previous experiments (intact: C7 from [17] and C1, respectively; amputee: C5 and C8, respectively), as part of experiments 3 and 4.

It can be suggested that the reason C6 is worse than other configurations is due to having fewer features (4 as oppose to 6 for C15, and 5 for C7 and C18). There is definite improvement for all mixed-domain configurations when measured against the best performing single-domain ones (TD=73.45% and DWT=73.47%), more so than for intact subjects (1.59% on average, compared to TD and 0.67% on average for DWT). This improvement could be considered negligible though plainly visible in Fig. 6. It indicates only a slight enhancement for amputee subjects when applying the additional wavelet transform process.

Combining TD and DWT features has improved classification accuracy for both intact and amputee subjects, with more benefit in the amputee data. The addition of a DWT process and subsequent STDCO and ENGCO features to the WL, RMS and SSC features has bolstered achieved accuracy, if not increased it significantly. This may question the validity of including the DWT, and whether the marginal gains outweigh the extra computation requirements. However, the small sample size here means the experiment may not be representative enough to say what are the best feature configurations and how good they are. Table 6 lists comparable work and shows a mixed outcome regarding the effectiveness of our best performing intact and amputee configurations against others' results. Differences in number of movements and subjects should certainly be accounted for when making an observation, indicating larger datasets prove challenging and provide more rigour during experiments.

4. Conclusion

This work continued a line of investigation into suitable sEMG feature configurations to accurately identify 17 human hand and wrist movements, using datasets from the NinaPro online repository. The focus was to build on previous TD work by incorporating features extracted from a DWT performed to 4 levels, using the Daubechies db7 wavelet, and to include testing with amputee data. Eighteen configurations were built of varying size, using features from the TD, the DWT, or a combination of both. Data from 11 intact and 9 amputee subjects were used for classification trials using a random forest classifier. Results show combining features from both domains increases classification accuracy for both subject types, with greater benefit evident in amputee data. A configuration consisting of RMS, WL, and SSC TD features and STDCO and ENGCO DWT features performed

Table 6. Comparison of configurations utilizing DWT feature extraction for both intact (Int) and amputee (Amp) subjects.

Reference	Moves	Chans	Subjects (Int, Amp)	Features	Wavelet & Levels	Acc. (%) (Int, Amp)
Al Omari et al. [1]	8	4	10, 0	Energy of DWT coeffs	sym4, 5	95.00, NA
Khezri & Jahed [11]	6	2	4, 0	MAV, SSC, AR coeffs, ZC of DWT coeffs	bior3.5, 9	92.00, NA
Duan et al. [5]	6	3	6, 2	MAV of DWT coeffs	coif5, 3	94.67, 85.17
Gijsberts et al. [7]	40	12	40, 0	RMS, HIST, mDWT, (Mean from Accelerometers)	db7, 3	82.49, NA
Atzori et al. [3]	50	12	40, 11	RMS, TD, HIST, mDWT	db7, 3	75.27, 46.27
This work	17	12	11, 9	RMS, WL, SSC, ENGCO, STDCO	db7, 4	90.98, 71.15

best (intact: 90.98%, amputee: 75.16%). The accuracy improvement over single domain configurations is only minor however, and a lack of any one dominant mixed-domain configuration (intact: 0.026% variance, amputee: 0.034% variance) suggests attempting to find an optimum set of features has limited scope in the current capacity. In terms of use for human-robot systems such as myoelectric control, it would be more apt to start with a solid base set of features and focus effort on improving or enhancing the machine learning method. This would require adapting to subject variation and the constant change in operating conditions. Our future work will investigate this sensitivity in sEMG-based systems, aiming to provide a solution with a suitable methodology that can adapt in real-time to subject needs and changes in operating environment.

5. ACKNOWLEDGMENTS

The sEMG data used in this paper are from the NinaPro project [3], we would like to express special thanks.

REFERENCES

[1] Al Omari, F. *et al*. 2014. Pattern recognition of eight hand motions using feature extraction of forearm emg signal. *Journal of Medical and Biological Engineering* 84, 3 (2014), 473–480.

[2] Atzori, M. *et al*. 2016. Effect of clinical parameters on the control of myoelectric robotic prosthetic hands. *Journal of Rehabilitation Research and Development* 53, 3, 345–358.

[3] Atzori, M. *et al*. 2014. Electromyography data for non-invasive naturally controlled robotic hand prostheses. *Scientific data* (2014), 1:140053. https://doi.org/10.1038/sdata.2014.53

[4] Chowdhury, S., and Nimbarte, A. 2015. Comparison of fourier and wavelet analysis for fatigue assessment during repetitive dynamic exertion. *Journal of Electromyography and Kinesiology* 25, 2 (2015), 205–213.

[5] Duan, F. *et al*., 2016. semg-based identification of hand motion commands using wavelet neural network combined with discrete wavelet transform. *IEEE Trans. Ind. Electron*. 63, 3, 1923–1934.

[6] Farina, D. *et al*. 2014. The extraction of neural information from the surface emg for the control of upper-limb prostheses: Emerging avenues and challenges. *IEEE Trans. Neural Syst. Rehabil. Eng*., 22, 4, 797–809.

[7] Gijsberts, A. *et al*. 2014. Movement error rate for evaluation of machine learning methods for semg-based hand movement classification. *IEEE Trans. Neural Syst. Rehabil. Eng*. 22, 4, 735–744.

[8] Gokgoz, E., and Subasi, A. 2015. Comparison of decision tree algorithms for emg signal classification using dwt. *Biomedical Signal Processing and Control* 18, 138–144.

[9] Hakonen, M, Piitulainen, H, and Visala, 2015. A. Current state of digital signal processing in myoelectric interfaces and related applications. *Biomedical Signal Processing and Control* 18, 334–359.

[10] Kakoty, N., Hazarika, S., and Gan, J. 2016. Emg feature set selection through linear relationship for grasp recognition. *Journal of Medical and Biological Engineering* 36, 6, 883–890.

[11] Khezri, M., Huang, H., and Jahed, M. 2011. A neuro-fuzzy inference system for semg-based identification of hand motion commands. *IEEE Trans. Ind. Electron*. 58, 1952–1960.

[12] Maier, J., Naber, A., and Ortiz-Catalan, M. 2018. Improved Prosthetic Control Based on Myoelectric Pattern Recognition via Wavelet-Based De-Noising. *IEEE Trans. Neural Syst. Rehabil. Eng*. 26, 2, 506-514.

[13] Nazmi, N. *et al*. 2016. A Review of Classification Techniques of EMG Signals during Isotonic and Isometric Contractions. *Sensors* 16, 8, 1–28.

[14] Oskoei A., and Hu, H. 2007. Myoelectric control systems-a survey. *Biomedical Signal Processing and Control* 2, 4, 275–294.

[15] Phinyomark, A., Kushaba, R.N., and Scheme, E.A. 2018. Feature Extraction Issue for Myoelectric Control Based on Wearable EMG Sensors. *Sensors* 18, 5, 1-17.

[16] Phinyomark, A. *et al*. 2013. Emg feature evaluation for improving myoelectric pattern recognition robustness. *Expert Systems with Applications* 40, 12, 4832–4840.

[17] Robinson, C. *et al*. 2017. Pattern classification of hand movements using time domain features of electromyography. *In Proceedings of the 4th International Conference on Movement Computing* (London, United Kingdom). MOCO '17. ACM, New York, NY, 27:1–6.

[18] Roche, A. *et al*. 2014. Prosthetic myoelectric control strategies: A clinical perspective. *Current Surgery Reports* 2, 3, 1–11.